# Automated scheduling of deferrable PEV/PHEV load in the smartgrid

Hongyuan Lu, Guodong Pang and George Kesidis
IE, CS&E and EE Depts
The Pennsylvania State University
{hzl142, gup3, gik2}@psu.edu

***Abstract*—We consider the scheduling of deferrable charging demand for plug-in electric or hybrid-electric vehicles (PEVs/PHEVs) in the smart grid such that the grid is operating within the safety charging threshold, and as many as consumers/users are satisfied by the end of a finite horizon (*e.g.*, 8pm-6am). Given that the charging profiles of PEVs/PHEVs are not constant and have a (truncated) prescribed triangle shape, the grid has to take into account such unevenness in the scheduling of their charging process. We assume that the consumers' charging profiles are known at the beginning of the finite horizon, and their charging can be interruptible. We develop an automated discrete-time scheduling algorithm in which the grid dynamically tracks the unevenness of each consumer's charging profile, and gives priority to consumers with highest unevenness that it can tolerate in each time period. For each consumer, the unevenness is measured by the cumulative difference of the charging profile and the average residual demand of his remaining charging profile in each time period until charging completion. This schedule is dynamic because it measures the average residual demand of each consumer in each time period. By comparing with an alternative scheduling algorithm that only measures the unevenness by the average demand of each consumer from their charging profile at the beginning, we show that the dynamic algorithm can better avoid bustiness in the charging process of the grid and can also satisfy much more consumers by the end of the finite horizon. We also compare with another algorithm, the SRPT algorithm, that gives priorities to consumers with shortest demand period, without taking into account unevenness. We conduct simulations to show the effectiveness of our scheduling algorithm in two scenarios: PEV/PHEV consumers, a mixture of PEV/PHEV consumers and constant-charging-profile consumers. With renewable energy supply, we allow the safety charging threshold to be random in each period and also conduct simulations to compare the performance of the algorithms in the scenario with mixed consumers.**

## I. Introduction

Plug-in electric or hybrid-electric vehicles (PEVs/PHEVs), as alternative vehicles, are recognized for their reducing greenhouse emissions and dependence on oil import related to national security concerns, so a growing number of PEVs/PHEVs is in need. By 2030, 6%-30% of vehicles in use will be PEVs/PHEVs; see, *e.g.*, [7]. Because of the increasing rate of PEV/PHEV adoption, the battery-charging of PEVs/PHEVs becomes a challenging question to the electric energy industry. This extra burden will explode if uncontrolled, because the time to charge most of PEVs/PHEVs, when people return home after work, coincides with the time of the peak of residential loads. In the context of efficient, robust and adaptive systems for electricity consumption, distribution and supply (*i.e.*, smart grids), home energy servers have been conceived to aid the individual residential consumer/user [15]. Though recent studies have shown that residential electricity consumption is generally not readily responsive to prices [15], perhaps the home energy servers will become more important in the future as it manages (on behalf of the typically sleeping consumer) the substantial overnight load due to charging of PEVs/PHEVs. Note that the collective capacity of PEVs/PHEVs may be ideally suited to exploit renewable wind energy supply which is often most plentiful at night; though wind energy is variable, it is short term predictable [2], [8]. Though our focus herein is *automated* charging of electric PEV/PHEV batteries in the early morning hours (a considerable collective load at a time-of-day when energy demands are presently least), we acknowledge that some PEV/PHEV battery charging may take place during the day at, say, specially equipped parking lots or, to a limited extent, by solar cell on the roof of the vehicle.

G. Kesidis was supported by NSF SaTC grant CCF-1228717 for this work.

In classical scheduling problems, jobs are typically assumed to be independently and identically distributed in size and duration, and arrive according to a prescribed stochastic, *e.g.*, Poisson process. Jobs are also typically not interruptible and constrained by limits on their sojourn times (queuing plus processing delays) in the system. Recently, scheduling problems for "smart" electrical grids have been given considerable attention by researchers. These problems typically fall into two broad categories: a centralized one where the grid itself largely controls the schedule of demand disclosed by the consumers, and a decentralized one where the grid only signals the consumers regarding the current spot price of power and the consumers decide their demand schedule. In this paper, we largely focus on a centralized problem setting for interruptible demand (typically as PEV/PHEV battery charging) with a collective finite time-horizon for charging (the start of the morning commute).

### A. Related Work

In [11], a day-ahead pricing strategy is set forth to move demand to off-peak hours. Their framework considers users' willingness to shift their demand and their numerical experiments are based on data from Ontario Hydro. However, studies have questioned the extent to which consumer behaviors can be thus manipulated by pricing [15].

In [19], a scheduling of interruptible and deferrable electric loads with renewable supplies is considered. All charging tasks have constant charging rates and individual deadlines. It is proved that no casual optimal scheduling policies exist and three coordinated algorithms (EDF, LLF, RHC) are compared through simulation-based tests. As electrical vehicles have different charging rates in different charging levels as mentioned in [1], in our paper, we focus on the scheduling of PEVs/PHEVs with unimodal peakedness charging profiles and there is a collective deadline for all consumers. From the current/voltage graph in [17] for LI-ion batteries [5], it should be noticed that the current is flat to a point and then diminishes; before that point, the voltage increases and then is flat afterwards; we deal with the resulting unimodal power-charging profile in the following.

One main feature of our paper is that charging is allowed to be both deferrable and interruptible. There are several papers on noninterruptible charging in the smart grid. In [4], an incentive-based energy consumption scheduling algorithm is proposed for the smart grid with consumers of noninterruptible constant demand profiles. In [13], such noninterruptible load/demand is considered in greater detail: consumer demand is assumed to arrive according to a Poisson process, is of constant power, and may be deferred up to an exponentially distributed service deadline (per consumer). Their objective is a long-term average cost function of instantaneous power consumed. Noninterruptible demand is also considered in [16], but there Poisson arrivals are due to an assumed mechanism to desynchronize demand (not the subject of policy optimization), the power profile is assumed unimodal, again consistent with that of the batteries of certain PEV/PHEV batteries [5], [17], [18], and all demand was assumed "available" at the start of a finite (*e.g.*, overnight) charging interval; demand was incrementally deferred to avoid overages. Specifically which consumers were deferred at a given time could be ascertained using a heuristic scoring system as for example given in [4].

In [4], [19], the focus is also on real-time scheduling of the power demand (tasks, jobs) of different consumers. Heuristic rules are given to prioritize consumers, *e.g.*, the "deferrable deadline" priority rule and scheduling via receding horizon control of an objective function inspired by (single) processor time allocation[1] in [19]. In [22], a "quality of experience" measure of power consumption is used in a collective objective function whose optimization is the aim of a consumer demand schedule.

In [20], a "network calculus" queuing model [3] is adapted to a broadly scoped power generation, distribution and demand system, including a somewhat aggregated model of consumer demand. The scheduling criterion we use in the following is related to the notion of "burstiness curve" of the network calculus literature.

### B. Problem setting

In summary, we assume deferrable and interruptible demand of non-constant power profile, where all demand is available at the start of a charging period and must be completed over a finite time-horizon ($T$), specifically modeling the task of charging PEV/PHEV batteries overnight. Instead of assuming that the grid signals spot prices to the consumers (based on a combination of current (real-time) demand and historical (*e.g.*, day ahead) demand), we assume that the consumers signal the grid (their demand aggregator, in particular) with their required charging profile[2]. A consumer's PHEV/PEV battery is connected to a circuit controlled by the grid[3]. We assume a fixed power budget ($L$) for a given community of consumers, instantaneous consumption above which is subject to overage charges (which are to be avoided if possible); The grid's task is then to schedule demand to avoid overages and to minimize the total unfulfilled charging by the end of the charging interval.

The presumption here is that this framework for PHEV/PEV battery charging will be cheaper for the consumer, compared to simply plugging their car into a circuit not controlled by the grid which results in charging that begins immediately (not deferred) and is not interrupted. These specific charging rates and the overage threshold $L$ are assumed to be informed by historical demand data and current prices of supply for the grid servicing the population of consumers considered in the following.

### C. Organization of the paper

This paper is organized as follows. In Section II, we describe a rule by which the grid can prioritize consumers so as to most likely meet all of their PEV/PHEV charging demands by the collective deadline. A summary of alternative approaches is given in Section III. A comparative numerical study is given in Section IV. We conclude in Section V with a summary.

## II. Scheduling by charging profile unevenness

### A. PEV Demand Profile

In [16], we studied PEV/PHEV demand profiles of unimodal type [5], [17], [18], an idealization of which is shown in Fig. 1. The power charging rate is approximated by a triangle-pulse function, $h(t)$, starting at time 0 with support $\eta > \zeta$ and peak value $H$ at time $\zeta$; see the top graph of Fig. 1. The $h(t)$ function has the following explicit expression

$$h(t;\eta,H,\zeta) = \begin{cases} \frac{H}{\zeta}t, & 0 \le t < \zeta, \\ -\frac{H}{\eta-\zeta}t + \frac{H\eta}{\eta-\zeta}, & \zeta \le t \le \eta. \end{cases} \quad (1)$$

With the help of Lithium-ion chemistry [5], batteries have no memory effect and can be recharged even when they are not discharged completely [9]. Thus, the power demand profile of a given smart grid PEV consumer at a given night may start with an arbitrary residual charge, and thus take the shape of the front-clipped (advanced) triangle pulse at the bottom of Fig. 1, *i.e.*,

$$h(t+\xi;\eta,H,\zeta)u(t),$$

[1] For which a common scheduling approach is simple earliest deadline first.

[2] In future work, we will consider the issue of the reliability of consumer attestation of demand for real-time and historically based pricing [10], [12], [14] for this setting.

[3] Such arrangements exist today for high-power applicances, particularly electric heaters and air conditioners, allowing the grid to briefly cycle power to these circuits in order to "peak-shave" demand.

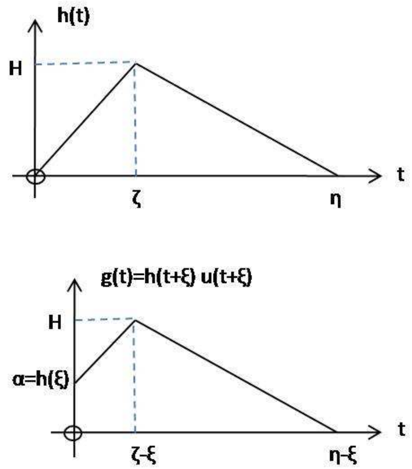


Fig. 1. Idealized PEV Battery Power Demand Charging Profile

where $u$ is Heaviside's unit-step function and $\xi > 0$ is the time corresponding to the amount of residual charge $\alpha = h(\xi)$. So, the PEV power consumption profile of the $i^{\text{th}}$ residential smart grid consumer is here parameterized by $(\tau_i, \xi_i, \eta_i, H_i, \zeta_i)$, where $\tau_i$ is the starting time of service request, *i.e.*,

$$g(t; \tau_i, \xi_i, \eta_i, H_i, \zeta_i) = h(t + \xi_i - \tau_i; \eta_i, H_i, \zeta_i) u(t - \tau_i).$$

### B. The Scheduling Algorithm

We consider a finite, discretized time-interval of length $T$ time-units, $\mathcal{I} := \{1, 2, ..., T\}$, and all consumer loads are "available" at the start of the interval and must be completed by the end. Suppose the $i^{\text{th}}$ consumer has a PEV/PHEV battery with required charging profile $g_i(1), g_i(1), ..., g_i(\eta_i)$ Joules/time-unit. The scheduled service times of the $i^{\text{th}}$ consumer are indicated by the process $s_i(t)$, $t \in \mathcal{I}$ (*cf.* the definition of $\mathcal{S}$ below). The mean power demand of the $i^{\text{th}}$ consumer is $\bar{g}_i(1) := \eta_i^{-1} \sum_{k=1}^{\eta_i} g_i(k)$.

We naturally assume a consumer will be charged in part according to their total energy consumption $(\bar{g}, \eta)$, equivalently according to their mean power consumption $(\bar{g})$ over the length of their period of consumption $(\eta)$. In addition, a consumer's charges may increase as a function of the degree of unevenness (burstiness) of user $i$'s charging; this can be defined as

$$\begin{aligned}
\sigma_i(t) &= \max_{-1 \le \rho \le r_i(t)-1} \sum_{k=s_i(t)}^{s_i(t)+\rho} [g_i(k) - \bar{g}_i(s_i(t))] \quad (2)\\
&= \max_{-1 \le \rho \le r_i(t)-1} \left( \sum_{k=s_i(t)}^{s_i(t)+\rho} g_i(k) \; - (\rho+1)\bar{g}_i(s_i(t)) \right) \quad (3)\\
&= \max \left\{ 0, \max_{0 \le \rho \le r_i(t)-1} \sum_{k=s_i(t)}^{s_i(t)+\rho} g_i(k) \; - (\rho+1)\bar{g}_i(s_i(t)) \right\}
\end{aligned}$$

where: $\sum_{k=s}^{s-1} x(k) \equiv 0$ for all $s$ and summands $x$ (so $\sigma_i(t) \ge 0 \; \forall i, t$), $g_i(k) = 0 \; \forall k > \eta_i$,

$$\begin{aligned}
\bar{g}_i(s_i(t)) &:= \frac{1}{r_i(t)} \sum_{k=s_i(t)}^{\eta_i} g_i(k),\\
r_i(t) &:= \eta_i - s_i(t) + 1.
\end{aligned}$$

Let $\mathcal{S}(t)$ be the set of users chosen for service at discrete-time $t \in \{1, 2, ..., T\}$. If $i \in \mathcal{S}(t)$, then $s_i(t+1) = s_i(t) + 1$ and $r_i(t+1) = r_i(t) - 1$.

Clearly, for feasible scheduling of all user demand without overages, we require that

$$TL \quad \ge \quad \sum_{i \in \mathcal{U}} \eta_i \bar{g}_i(1), \qquad (4)$$

where $\mathcal{U}$ is the set of consumers/users, and

$$r_i(1) = \eta_i \quad \text{and} \quad s_i(1) = 1 \;\; \forall i \in \mathcal{U}.$$

Of course, (4) might not suffice for schedulability.

Assuming (4), we propose to schedule by priority based on residual demand-unevenness $\sigma_i$ with ties broken by either the maximum of residual mean power demand $\bar{g}_i(s_i)$ or the maximum charging demand $g_i^{\max}(s_i)$, where $g_i^{\max}(s_i(t)) = \max_{s_i(t) \le k \le \eta_i, \; i \in \mathcal{U}} \{g_i(k)\}$. That is, for all $t$, $\mathcal{S}(t)$ satisfies:

- $\sum_{i \in \mathcal{S}(t)} g_i(s_i(t)) \le L$,
- for all $j \notin \mathcal{S}(t)$,
  - $\sigma_j(t) \le \min_{i \in \mathcal{S}(t)} \sigma_i(t)$,
  - if $\sigma_j(t) = \sigma_i(t)$ for some $i \in \mathcal{S}(t)$, either

    **(M1)** : $\bar{g}_j(s_j(t)) \le \bar{g}_i(s_i(t))$,

    *or*

    **(M2)** : $g_j^{\max}(s_j(t)) \le g_i^{\max}(s_i(t))$.

### C. Measure of Total Unevenness

As a measure of total residual work difficulty, define

$$B(t) \quad := \quad \sum_{i \in \mathcal{U}} \sigma_i(t).$$

First note that if $i \in \mathcal{S}(t)$, then

$$\bar{g}_i(s_i(t)) = \frac{r_i(t) - 1}{r_i(t)} \bar{g}_i(s_i(t+1)) + \frac{1}{r_i(t)} g_i(s_i(t)), \qquad (5)$$

where, again, $r_i(t+1) = r_i(t) - 1$ and $s_i(t+1) = s_i(t) + 1$. So,

$$\begin{aligned}
\sigma_i(t) = \max \Big\{ & 0, \; g_i(s_i(t)) - \bar{g}_i(s_i(t)) \\
& + \max_{-1 \le \rho' \le r_i(t+1)-1} \sum_{k=s_i(t+1)}^{s_i(t+1)+\rho'} [g_i(k) - \bar{g}_i(s_i(t))] \Big\},
\end{aligned}$$

where the "0" term corresponds to $\rho = -1$ in (2) and we have substituted $\rho' = \rho - 1$. By (5), if $i \in \mathcal{S}(t)$, then

$$\sigma_i(t) \ge \max \left\{ 0, \; \frac{2}{r_i(t)} g_i(s_i(t)) - \bar{g}_i(s_i(t)) + \sigma_i(t+1) \right\}; \quad (6)$$

otherwise, $\sigma_i(t+1) = \sigma_i(t)$. If the relation in (6) was equality, this would be a Lindley recursion (as describing the dynamics of a queue's backlog, [21]). Clearly by (6),

$$B(t+1) \quad \le \quad \tilde{B}(t+1), \qquad (7)$$

where the upper bound

$$\tilde{B}(t+1) := B(t) - \sum_{i\in\mathcal{S}(t)} \left[\frac{2}{r_i(t)} g_i(s_i(t)) - \bar{g}_i(s_i(t))\right].$$

We can relax the lower bound in (6) further by the following

$$\sigma_i(t) \geq \max\left\{0,\ \frac{2}{\bar{\eta}} g_i(s_i(t)) - \bar{g}_i(s_i(t)) + \sigma_i(t+1)\right\}, \quad (8)$$

where $\bar{\eta} := \max_i \eta_i$. Thus, if

$$\sum_{i\in\mathcal{S}(t)} g_i(s_i(t)) \quad \approx \quad L, \quad (9)$$

*i.e.*, assuming sufficient demand and a large user population so that $g_i(k) \ll L$ for all $i, k$, then (7) becomes

$$B(t+1) \quad \leq \quad \hat{B}(t+1), \quad (10)$$

where the upper bound

$$\hat{B}(t+1) := B(t) - \frac{2}{\bar{\eta}} L + \sum_{i\in\mathcal{S}(t)} \bar{g}_i(s_i(t)).$$

So, we have shown:

*Theorem 2.1:* If at time $t$:

- $\sigma_i(t)$ are given for all $i \in \mathcal{U}$,
- (9) holds, and
- scheduling by $\sigma_i$ priority, with ties broken by $\bar{g}_i(s_i)$,

then $\hat{B}(t+1)$ is (obviously) minimized with

$$\hat{B}(t+1) \quad \geq \quad B(t+1).$$

Note that it's also possible to choose $\mathcal{S}(t)$ so as to directly minimize $B(t+1)$; but this requires a large combinatorial search that is greatly simplified by a priority rule. We also note that the measure $B(t)$ remains the same for the two methods **M1** and **M2**, and so do the two upper bounds $\tilde{B}(t)$ and $\hat{B}(t)$. Finally note that this scheduling criterion is similar to the "service curve" [3].

## III. Alternative scheduling criteria

We now introduce two alternative scheduling methods. First, different variations of (2) are readily considered, *e.g.*, by simply replacing the residual mean power requirement $\bar{g}_i(s_i(t))$ with the initial mean power requirement spread out over the whole charging interval $e_i := \eta_i \bar{g}_i(1)/T$. Thus, we have

$$\begin{aligned} \sigma_i(t) &= \max_{-1\leq\rho\leq r_i(t)-1} \sum_{k=s_i(t)}^{s_i(t)+\rho} [g_i(k) - e_i] \quad (11) \\ &= \max\left\{0, \max_{0\leq\rho\leq r_i(t)-1} \sum_{k=s_i(t)}^{s_i(t)+\rho} g_i(k) \ - (\rho+1)e_i\right\} \end{aligned}$$

This leads to an exact Lindley recursion for $\sigma_i$ when $i$ is scheduled,

$$\sigma_i(t) \quad = \quad \max\{0,\ g_i(s_i(t)) - e_i + \sigma_i(t+1)\}.$$

Similar to **(M1)** and **(M2)**, we use the scheduling approach in Section II by priority based on residual demand unevenness $\sigma_i$ with ties broken by either the average of total demand $e_i$ or the maximum charging demand $g_i^{\max}(s_i)$. That is to say, if $\sigma_j(t) = \sigma_i(t)$ for some $i \in \mathcal{S}(t)$ and for all $j \notin \mathcal{S}(t)$, either

**(M3)** : $e_j \leq e_i$,
*or*
**(M4)** : $g_j^{\max}(s_j(t)) \leq g_i^{\max}(s_i(t))$.

We next introduce a scheduling method that simply gives priority to consumers with the shortest remaining processing (demand) time (SRPT) at each scheduling time slot, without taking into account the demand profile unevenness. That is, for all t, $\mathcal{S}(t)$ satisfies:

- $\sum_{i\in\mathcal{S}(t)} g_i(s_i(t)) \leq L$,
- for all $j \notin \mathcal{S}(t)$,
  - $\max_{i\in\mathcal{S}(t)} r_i(t) \leq r_j(t)$,
  - if $r_j(t) = r_i(t)$ for some $i \in \mathcal{S}(t)$, we randomly choose either customer $i$ or $j$.

## IV. Numerical results

We now present results of numerical experiments to illustrate the performance of our scheduling algorithm in Section II and compare with the two alternative scheduling algorithms in Section III.

### A. Only PEV/PHEV Consumers

First, an input data set of consumer demand charging profiles as in Fig. 1 was generated according to the following random mechanism. We chose $N = 1000$, $T = 480$ minutes, $H \sim \mathsf{Uniform}(50, 100)$, $\eta \sim \mathsf{Uniform}(60, 120)$, $\zeta|\eta \sim \mathsf{Uniform}(0, \eta)$ and $\xi|\zeta \sim \mathsf{Uniform}(0, \zeta)$. For this particular data set, the critical value of $L$ in (4) is given by $L = 5986$.

We implemented the three scheduling algorithms for this consumer demand portfolio data set. We next show the performance of our algorithm of Section II. Fig. 2 depicts the total unevenness measure $B(t)$ and its two upper bounds $\tilde{B}(t)$ and $\hat{B}(t)$. We see that the two upper bounds are both very tight[4].

In Fig. 3, we compare the total unevenness measure $B(t)$ of our scheduling algorithm in Section II with the first alternative scheduling algorithm (**M3**) in Section III. It is evident that the total unevenness measure $B(t)$ of our algorithm is much smaller than that of the alternative one. This shows that our algorithm is very effective in reducing the unevenness by taking into account the progressive peakedness in the future at each time instead of simply using the peakedness measure over the entire demand period.

It is clear that our scheduling algorithm is not work-conserving, that is, some residual supply may not be utilized at some time. This may be desirable in order to avoid demand overages. We compare the residual supply (headroom room to the overage threshold $L$) at each time of our scheduling algorithm with that of the alternative algorithms. Let $X(t) =$

[4]Note that the plot shows the results for the **M1** method, but as we have noted, methods **M1** and **M2** give the same schedule.

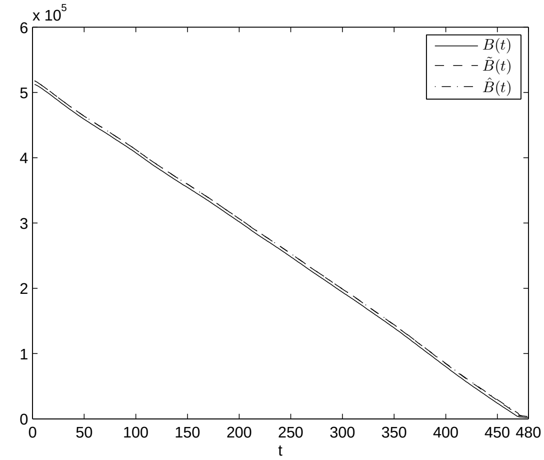


Fig. 2. Comparison of $B(t)$, $\tilde{B}(t)$ and $\hat{B}(t)$ under scheduling using profile unevenness (Schedule 1).

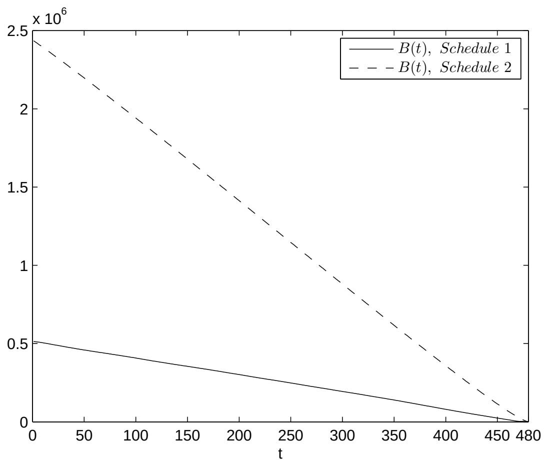


Fig. 3. Comparison of $B(t)$ under Schedule 1 and Schedule 2.

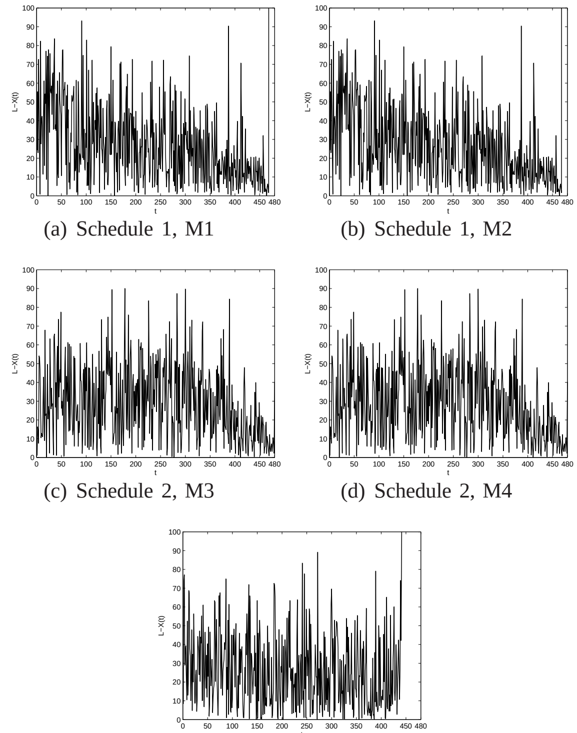


(a) Schedule 1, M1 (b) Schedule 1, M2

(c) Schedule 2, M3 (d) Schedule 2, M4

(e) SRPT

Fig. 4. The headroom $R(t) = L - X(t)$ (a) for M1, (b) for M2, (c) for M3, (d) for M4 and (e) for SRPT.

$\sum_{i\in\mathcal{S}(t)} g_i(s_i(t))$ be the amount of energy that are consumed at time $t$. The headroom $R(t) = L - X(t)$ at each time $t$ is depicted in Fig. 4. From these plots, we see that all these algorithms result in some residual supply most of the time. The headroom under our scheduling algorithm shows a clear decreasing trend in Fig. 4 (a) and (b). We observe a similar but less clear trend in our second scheduling algorithm; see Fig. 4 (c) and (d). However, the SRPT algorithm does not seem to have this feature, as shown in Fig. 4 (e). Note that after a given point in time ($T_0$), the headroom $R(t)$ may become large enough to exceed the maximum value of any consumer's charging profile, see Fig. 4 (a), (b) and (e), while such a phenomenon is absent in Fig. 4 (c) and (d). This is because not many consumers are remaining in the system after that point in time under our "Schedule 1" (Section II) or SRPT algorithms, consumer demand needs to be satisfied in order of the demand charging profile, and not-completely satisfied consumers remained at the end of the charging interval $T$ under "Schedule 2" (Section III) algorithms; see the following tables.

In addition, we used the following three performance measures (P.M.) to compare these scheduling algorithms:

1) The average headroom to the threshold,

$$V_1 := \frac{1}{T_0}\sum_{t=1}^{T_0} R(t) = \frac{1}{T_0}\sum_{t=1}^{T_0}(L - X(t));$$

where $T_0$ is the last time when the headroom $R(t)$ is less or equal to the maximum value of any consumer's charging profile. In the above numerical example, $T_0 = \sup\{t \geq 1 : (L - X(t)) \leq 100\}$, where 100 is the upper bound of the charging profile of all consumers.

2) The total residual demand,

$$V_2 := \sum_{i\in\mathcal{U}} r_i(T)\bar{g}_i(s_i(T));$$

3) The number of consumers who do not finish their service at time $T$ (*i.e.*, are not completely satisifed),

$$V_3 := \sum_{i\in\mathcal{U}} \mathbb{1}\{s_i(T) \leq \eta_i\},$$

where $\mathbb{1}$ is an indicator function: $\mathbb{1}\{A\} = 1$ when the event $A$ occurs and $\mathbb{1}\{A\} = 0$ otherwise.

These three performance measures were evaluated and are given in Table I. First, observe that the two methods of Schedule 1 gave similar performance, and similarly the two methods of Schedule 2. All approaches gave relatively small $V_1$, implying that the utilizations under all scheduling algorithms were relatively high. Schedule 1 performed better than SRPT, with less total residual demand and fewer not completely satisfied consumers, and Schedule 1 outperformed Schedule 2 in terms of not completely satisfied consumers, even though the total residual demand under Schedule 2 was smaller than that under Schedule 1.

| P.M. | Schedule 1 | | Schedule 2 | | SRPT |
|---|---|---|---|---|---|
| | M1 | M2 | M3 | M4 | |
| $V_1$ | 26.9100 | 26.9100 | 28.7538 | 28.7538 | 24.8821 |
| $V_2$ | 57874.79 | 57874.79 | 13789.52 | 13789.52 | 68153.58 |
| $V_3$ | 35 | 35 | 800 | 800 | 86 |

TABLE I
COMPARISON OF PERFORMANCE MEASURES FOR THE SCHEDULING ALGORITHMS.

### B. Two Types of Consumers

A demand aggregator may also have to deal with flexible loads which have a constant charging rate $H_c$, such as air conditioners, electric heaters, and washing machines. To check how our algorithms perform under a mixture of these two types of consumers, we also generated a second type of consumer with $H_c = 50$ and the charging time $\eta \sim \mathsf{Uniform}(60, 120)$. These two types of consumers were in equal proportion. The number of not completely satisfied consumers for the first type and the second type are respectively denoted $V_3^{(1)}$ and $V_3^{(2)}$. An input data set of consumer demand charging profiles was generated and we chose $L = 7641$ as before for the data set.

Numerical results, given in Table II, again show that the two methods **M1** and **M2** of Schedule 1 had approximately the same performance measures, and similarly for the two methods **M3** and **M4** of Schedule 2. For the measures of $V_1$ and $V_2$, Schedule 1 outperformed SRPT; in particular, Schedule 1 finished all PEV consumers' charging requirement while SRPT had nine not completely satisfied PEV consumers, which verifies that our algorithm gives priority to consumers with uneven demand profiles. We also observe that Schedule 2 had a large amount of not completely satisfied consumers even though the total residual demand was smaller than that under Schedule 1.

| P.M. | Schedule 1 | | Schedule 2 | | SRPT |
|---|---|---|---|---|---|
| | M1 | M2 | M3 | M4 | |
| $V_1$ | 31.3366 | 31.3425 | 25.4380 | 25.4380 | 25.5803 |
| $V_2$ | 98950.00 | 98950.00 | 16541.09 | 16541.09 | 122430.54 |
| $V_3^{(1)}$ | 0 | 0 | 422 | 422 | 9 |
| $V_3^{(2)}$ | 74 | 74 | 0 | 0 | 74 |

TABLE II
COMPARISON OF PERFORMANCE MEASURES FOR THE SCHEDULING ALGORITHMS.

### C. Two Types of Consumers with Renewable Power Supply

Renewable energy is playing an increasingly important role in supplying power to consumers. Solar and wind [2] constitute 2% of the electricity generated in the US in 2009, and it is expected that 30% of total electricity supply will come from renewables by 2030 [6].

Assuming that a proportion of the grid's power comes from the renewable energy, the overage threshold $L$ is now time-varying: $L = \bar{L}^* + L_0$, where $\bar{L}^*$ is the grid's (constant) overage threshold from the conventional supply, and $L_0$ represents renewable supply process assumed to be Gaussian distributed with i.i.d. marginals $L_0 \sim N(\mu_0, \sigma_0^2)$. Using the same data set of consumers' demand-profiles as in Section IV-B, we get $L^* = 7640.31$ from (4). We chose $\bar{L}^* = 0.9L^* = 6876.28$, $\mu_0 = 0.1L^* = 764.03$ and $\sigma_0 = 0.2\mu_0 = 152.81$.

The numerical results are given in Table III. Again, we see that the two methods **M1** and **M2** of Schedule 1 had approximately the same performance measures, and similarly for the two methods **M3** and **M4** in Schedule 2. Schedule 1 outperforms SRPT. In particular, Schedule 1 had finished all PEV/PHEV consumers' charging requirement, while SRPT had nine not completely satisfied PEV/PHEV consumers. Renewable energy, as the supplementary supply of the power to the smart grid, indeed enhanced the performance of all approaches: compare total residual demand in Table II and Table III. It is also observed that, even though the total residual demand under Schedule 2 is smaller than that under Schedule 1, there are still more not completely satisfied consumers under Schedule 2 than that under Schedule 1.

| P.M. | Schedule 1 | | Schedule 2 | | SRPT |
|---|---|---|---|---|---|
| | M1 | M2 | M3 | M4 | |
| $V_1$ | 24.3625 | 24.3334 | 27.7019 | 27.7019 | 25.7367 |
| $V_2$ | 91700.00 | 91800.00 | 13024.99 | 13024.99 | 118734.47 |
| $V_3^{(1)}$ | 0 | 0 | 390 | 390 | 9 |
| $V_3^{(2)}$ | 72 | 71 | 0 | 0 | 74 |

TABLE III
COMPARISON OF PERFORMANCE MEASURES FOR THE SCHEDULING ALGORITHMS.

## V. CONCLUSIONS

We considered the scheduling of deferrable and interruptible PEV/PHEV battery-charging load in a smart grid for two scenarios: only PEV/PHEV consumers, and a mixture of PEV/PHEV consumers and constant-charging-profile consumers. By numerical experiments, we showed how our proposed automated scheduling algorithm (Schedule 1) can satisfy much more consumers compared to other alternative approaches in both cases. Since SRPT only focuses on the remaining charging time without considering peakedness/unevenness of each consumer's charging profile, it performed worst in the sense that both the total unfulfilled demand and the number of not completely satisfied consumers (at the end of the charging period). Although the alternative Schedule 2 can reduce the total residual demand efficiently, there are still many not completely satisfied consumers, especially in the case of only PEV/PHEV consumers. With a supply of renewable energy, Schedule 1 is also shown to significantly decrease the number of not completely satisfied consumers.

## REFERENCES

[1] S. Argade, V. Aravinthan, and W. Jewell. Probabilistic modeling of EV charging and its impact on distribution transformer loss of life. In *Proc. IEEE Int'l Electric Vehicle Conference (IEVC)*, April 2012.

[2] European Wind Energy Association. Wind energy: The facts. part 2, chapter 2 - understanding variable output characteristics of wind power. http://www.wind-energy-the-facts.org/en/part-2-grid-integration, 2009.

[3] J. Boudec and P. Thiran. Network calculus: A theory of deterministic queueing systems for the Internet. *Online version of the Book Springer Verlag - LNCS 2050*, April 2012.

[4] S. Caron and G. Kesidis. Incentive-based energy consumption scheduling algorithms for the smart grid. In *Proc. IEEE SmartGridComm*, Gaithersburg, MD, Oct. 2010, Extended version http://www.cse.psu.edu/∼kesidis/papers/smartgridcomm10-extended.pdf.

[5] Tesla Motors Company. Roadster innovations/battery: Increasing energy density means increasing range. Available at http://www.teslamotors.com/roadster/technology/battery.

[6] G. Crabtree, J. Misewich, R. Ambrosio, K. Clay, P. Demartini, R. James, M. Lauby, V.Mohta, J. Moura, P. Sauer, F. Slakey, J. Lieberman, and H. Tai. Integrating renewable electricity on the grid:a report by the aps panel on public affairs. *APS*, November 2010.

[7] EPRI. Impact of plug-in electric vehicle technology diffusion on electricity infrastructure: Preliminary analysis of capacity and economic impacts. product id # 1016853, 2010, http://mydocs.epri.com/docs/Portfolio/PDF/2010_P018.pdf.

[8] M. Galus, R. Fauci, and G. Andersson. Investigating PHEV wind balancing capabilities using heuristics and model predictive control. In *Proc. IEEE PES General Meeting*, 2010.

[9] How to prolong lithium-based batteries. Available at http://batteryuniversity.com/learn/article/how_to_prolong_lithium_based_batteries.

[10] L. Jia, R.J. Thomas, and L. Tong. Malicious data attack on real-time electricity market. In *Proc. IEEE Int'l Conf. on Acoustics, Speech and Signal Processing (ICASSP)*, May 2011.

[11] C. Joe-Wong, S. Sen, S. Ha, and M. Chiang. Optimized day-ahead pricing for smart grids with device-specific scheduling flexibility. *IEEE JSAC*, July 2012.

[12] O. Kosut, L. Jia, R.J. Thomas, and L. Tong. Malicious data attacks on smart grid state estimation: attack strategies and countermeasures. In *Proc. IEEE SmartGridComm*, Gaithersburg, MD, Oct. 2010.

[13] I. Koutsopoulos and L. Tassiulas. Optimal control policies for power demand scheduling in the smart grid. *IEEE JSAC*, July 2012.

[14] Y. Liu, P. Ning, and M. Reiter. False data injection attacks against state estimation in electric power grids. *ACM Transactions on Information and Systems Security (TISSEC)*, 14(1), May 2011.

[15] M. Mosko and V. Bellotti. Smart conservation for the lazy consumer. *IEEE Spectrum*, July 2012.

[16] G. Pang, G. Kesidis, and T. Konstantopoulos. Avoiding overages by deferred aggregate demand for PEV charging on the smart grid. In *Proc. IEEE ICC Selected Areas in Communications Symposium: Smart Grids*, June 2012, Extended version http://www.cse.psu.edu/research/publications/tech-reports/2011/CSE-11-009.pdf.

[17] IBT power. Lithiumion technical data, 2012, Available at http://www.ibt-power.com/Battery_packs/Li_Ion/Lithium_ion_tech.html.

[18] C. Simpson. Battery charging. *National Semiconductor*, 2011, Available at http://cegt201.bradley.edu/projects/proj2008/lcc/pdf/national_battery_charging.pdf.

[19] A. Subramanian, M. Garcia, A. Dominguez-Garcia, D. Callaway, K. Poolla, and P. Varaiya. Real-time scheduling of deferrable electric loads. In *Proc. American Control Conference (ACC)*, 2012.

[20] K. Wang, F. Ciucu, C. Lin, and S.H. Low. A stochastic power network calculus for integrating renewable energy sources into the power grid. *IEEE JSAC*, July 2012.

[21] R.W. Wolff. *Stochastic Modeling and the Theory of Queues*. Prentice Hall, 1989.

[22] L. Zhou, J.J.P.C. Rodrigues, and L.M. Oliveira. QoE-driven power scheduling in smart grid: Architecture, strategy, and methodology. *IEEE Commun. Mag.*, May 2012.